



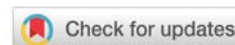
Submitted : 15 May, 2026
Accepted : 05 June, 2026
Published : 06 June, 2026

***Corresponding author:** A.V. Stepanov, Belorussian State University (BSU), National Ozone Monitoring Research and Educational Center (NOMREC), 7-816 Kurchatov Street, 220045, Minsk, Republic of Belarus, E-mail: stepav54@mail.ru

Keywords: Algorithm for electromagnetic frequencies; That may create stability of biological order; Resonant recognition model; Activation process model; Protein energy landscapes; Dipole moments of electronic transitions

Copyright License: © 2026 Stepanov AV, et al. This is an open-access article distributed under the terms of the Creative Commons Attribution License, which permits unrestricted use, distribution, and reproduction in any medium, provided the original author and source are credited.

<https://www.chemisgroup.us>



Review Article

Protein energy landscapes exploration by means of the activation process model

AV Stepanov^{1*}, MA Stepanov²

¹Belorussian State University (BSU), National Ozone Monitoring Research and Educational Center (NOMREC), 7-816 Kurchatov Street, 220045, Minsk, Republic of Belarus

²Department of Technical Physics. Information Technologies and Robotics Faculty, Belarusian National Technical University, B. Khmel'nitsky str. 9, Building 11, 220013 Minsk, Belarus

Abstract

The activation process model is used to explain energy transfer in proteins for energies less than 1 eV. The model does not require the use of quasi-particles, like phonons, excitons, or solitons. As a protein molecule absorbs electromagnetic energy, electronic transitions take place by means of activation processes associated with various conformational substates of a protein. This leads to resonances in various frequency ranges, including THz, GHz, MHz, and kHz. The resonances are explored for tubulins, several telomerases and telomeres, and ion channel proteins related to pain transmission.

Introduction

Any living cell absorbs electromagnetic waves resonantly in a fairly wide frequency range. This amazing feature was studied extensively by Hans J. H. Geesink and Dirk K. F. Meijer [1]. They proposed a hypothesis of a mathematical algorithm for electromagnetic frequencies that may create stability of biological order. Using this algorithm, they developed a bio-soliton model capable of predicting non-thermal electromagnetic radiation frequency bands that could either stabilize or destabilize life conditions [2].

Another model for the calculation of electromagnetic resonances in proteins was proposed by Irena Cosič. This is the resonant recognition model (RRM) [3]. The RRM is based on the finding that certain frequencies within the distribution of energies of delocalized electrons along a protein molecule are critical for protein biological function and/or interaction with its target. The RRM enables these frequency characteristics to be calculated. First, the protein primary structure is

presented as a numerical series by assigning the electron-ion interaction pseudopotential relevant to the protein's biological activity to each amino acid. Second, the numerical series are analyzed by digital signal analysis methods, using inverse Fourier transform and wavelet transform, in order to extract information pertinent to the biological function. Each RRM frequency characterizes one particular biological function or interaction [4]. The in-depth model description and RRM frequencies for various proteins can be found in [5].

From the physics of electron transitions standpoint, both models treat optical resonances identically. That is not the case for gigahertz, megahertz, and kilohertz resonance frequencies. These are explained in terms of phonons, excitons, and solitons. However, these quasi-particles are used differently. For example, solitons transfer energy along alpha-helices only [6], or through the entire volume of a protein [7].

Apparently, it is still not entirely clear how exactly the process of energy transfer by means of electromagnetic resonances occurs in proteins [8,9]. Assume this process results

from an activation process taking place on one of the protein energy landscapes. Let us consider this problem in detail.

Protein energy landscapes

It is known that proteins possess a complex energy landscape with a large number of local minima called conformational substates (CS) that are arranged in a hierarchical fashion [10]. Daniël Thorn Leeson used flash photolysis and spectral diffusion to study the dynamics of CO molecule bond restoration in Zn-myoglobin heme in the range from 100 mK to 300K [11]. He derived the following sequence for CS tiers: $CS_4 \leq 9.1 \cdot 10^{-4}$ eV, $CS_3 \leq 0.01$ eV, $CS_2 \leq 0.1$ eV, $CS_1 \leq 1.0$ eV, and $CS_0 > 1.0$ eV. To understand what kind of activation processes arise, one has to calculate the frequency of thermal radiation ν_{\max} at which the exchange of energy between radiation and a molecule is most efficient [12]. The value of ν_{\max} for $T=100$ mK is $5.875 \cdot 10^9$ Hz, and the one for $T=300$ K is $1.763 \cdot 10^{13}$ Hz. The corresponding values of thermal radiation quanta are $2.432 \cdot 10^{-5}$ eV and $7.299 \cdot 10^{-2}$ eV.

Thus, activation processes caused by thermal equilibrium radiation can occur on CS_4 , CS_3 , and CS_2 tiers. Then it would be reasonable to conclude that non-equilibrium activation processes take place on CS_1 and CS_0 tiers. Energy released by the hydrolysis of adenosine triphosphate (ATP) to adenosine diphosphate (ADP) and inorganic phosphate is enough for CS_2 and CS_1 activation processes, while light activates biochemical reactions on the CS_0 tier [13].

According to Aristotle, nature does nothing uselessly. Myoglobin is sometimes called a hydrogen atom in biology [14]. Using Occam's razor, it is tempting to generalize D.T. Leeson's energy landscape estimates to more complex macromolecules such as tubulin protein [15,16], telomerase, telomere as an example of DNA, and TERT mRNA [17], and ion channel proteins related to pain transmission [18].

The resonant recognition model was used in [16-18] to calculate RRM frequencies for the proteins under consideration. Now we use the activation process model to interpret these frequencies.

Activation process model

The model is based on two assumptions:

- (1) In elementary activation interaction act, potential energy of moving atoms changes discretely or in quanta. The elementary activation act appears to be a series of quantum subsystems occurring in sequence. These subsystems can also be defined as identical quantum oscillators.
- (2) Energy exchange between electromagnetic radiation and interacting atoms results in discrete translational motion changes of those atoms that absorb and subsequently emit an oscillation energy quantum series [19-21].

With these assumptions in mind, the average energy of activation process is calculated as

$$\varepsilon_m = \frac{h\nu}{e^{mh\nu/kT} - 1}, \quad (1)$$

Here, m is the number of subconformations that a protein forms when passing the activation barrier on a given tier, ν is the frequency characterizing the quantum oscillator, $mh\nu = h\nu_a$ is the activation energy for the barrier. The value of ν equals the Einstein spontaneous emission coefficient A [22], so subconformations' lifetimes are inversely proportional to it. Consequently, one can get the unimolecular reaction rate constant as

$$K = \frac{\varepsilon_m}{h} = \frac{h\nu}{e^{mh\nu/kT} - 1}. \quad (2)$$

Suppose that each tier is associated with several coexisting activation processes, their activation energies being within the tier's energy range. The main model parameters in Eqs (1-2) are ν and $\nu_a = m\nu$. The number of quantum subsystems m forming a barrier is of the order of 10^5 - 10^6 for low-temperature equilibrium fluctuations of myoglobin [23,24] as well as for non-equilibrium L-lactate dehydrogenase catalytic reactions for reversible reduction of pyruvate to L-lactate *in vivo* [25]. It would be reasonable to suggest the same order of m for the proteins under investigation. In addition, the radiation of interest, by its nature, is associated with dipoles. Their dipole moments can be derived using the known formula [22]:

$$\vec{D} = 0.5 \cdot \sqrt{\frac{\nu \cdot (137)^3}{m \cdot \nu}} (\hat{A}). \quad (3)$$

It was previously demonstrated that these values should fall in the range 1 to 2 Å [25].

Tubulin

Tubulin is a protein that exists in all eukaryotic cells. It is polymerized as a dimer of alpha and beta molecules. These dimers are then polymerized into long filaments called microtubules. Their conductivity depends on whether they are filled with water or not. Microtubules are essential for cell movement, intracellular transport, cell division, and synaptic plasticity in brain neurons. However, the mechanisms by which microtubules organize intracellular dynamics are still not known.

A meticulously conducted, comprehensive experimental study of microtubules derived from pig brain uncovered several resonant frequencies in various regions of the electromagnetic spectrum [15]. In [16], the RRM method was applied to a variety of tubulins, namely rat, pig, human, mouse, and bovine ones. The RRM frequencies analysis revealed a striking commonality in the functioning of microtubules regardless of the mammal species.

Mean values of these RRM frequencies are now used to calculate all necessary parameters for the activation process model. They are presented in Tables 1-4. Column 6 shows tiers for activation barriers. Columns 7 and 8 demonstrate

**Table 1:** Main parameters for frequency couple $10^{14}\text{Hz}/10^9\text{Hz}$ of tubulin.

RRM Frequency	Optical range (IR) ν 10^{14} Hz (Cosic)	Radio frequency range (Microwave) ν_0 10^9 Hz (Yomosa)	$m=\nu/\nu_0$	D (A°)	$\Delta E=mh\nu_0$ (eV)	Tier	$K_{T=298}$	$K_{T=314}$
0.0957	0.99	0.4015	246575	1.61464	$4.0943167 \cdot 10^{-1}$	CS ₁	$4.77901 \cdot 10^1$	$1.07683 \cdot 10^2$
0.3320	3.43	1.398	245351	1.61867	1.418536	CS ₀	$1.4292 \cdot 10^{-15}$	$2.38525 \cdot 10^{-14}$
0.4346	4.49	1.799	249583	1.60488	1.8569174	CS ₀	$7.09036 \cdot 10^{-23}$	$2.82417 \cdot 10^{-21}$
0.0234	0.24	0.0975	246154	1.61602	$9.9256161 \cdot 10^{-2}$	CS ₂	$2.0435 \cdot 10^6$	$2.48834 \cdot 10^6$

Table 2: Main parameters for frequency couple $10^{13}\text{Hz}/10^8\text{Hz}$ of tubulin.

RRM Frequency	Optical range (IR) ν 10^{13} Hz (Yomosa)	Radio frequency range (Short waves) ν_0 10^8 Hz (Ichinose)	$m=\nu/\nu_0$	D (A°)	$\Delta E=mh\nu_0$ (eV)	Tier	$K_{T=298}$	$K_{T=314}$
0.0957	1.5	0.41	365854	1.32555	$6.2035161 \cdot 10^{-2}$	CS ₂	$3.66134 \cdot 10^6$	$4.14095 \cdot 10^6$
0.3320	6.8	1.94	350515	1.35425	$2.8122579 \cdot 10^{-1}$	CS ₁	$3.40161 \cdot 10^3$	$5.94339 \cdot 10^3$
0.4346	6.8	1.94	350515	1.35425	$2.8122579 \cdot 10^{-1}$	CS ₁	$3.40161 \cdot 10^3$	$5.94339 \cdot 10^3$
0.0234	0.4	0.1	400000	1.26771	$1.6542694 \cdot 10^{-2}$	CS ₂	$5.25084 \cdot 10^6$	$5.42606 \cdot 10^6$

Table 3: Main parameters for first frequency couple $10^{10}\text{Hz}/10^5\text{Hz}$ of tubulin.

RRM Frequency	Radio frequency range (Microwave) ν 10^{10} Hz (Davydov)	Radio frequency range (Long waves) ν_0 10^5 Hz (Ichinose)	$m=\nu/\nu_0$	D (A°)	$\Delta E=mh\nu_0$ (eV)	Tier	$K_{T=298}$	$K_{T=314}$
0.0957	2.15	0.61	352459	1.35051	$8.8916978 \cdot 10^{-5}$	CS ₄	$6.07891 \cdot 10^4$	$6.07999 \cdot 10^4$
0.3320	9.95	2.19	469340	1.17033	$4.114995 \cdot 10^{-4}$	CS ₃	$2.08630 \cdot 10^5$	$2.08800 \cdot 10^5$
0.4346	9.95	2.78	357914	1.34018	$4.114995 \cdot 10^{-4}$	CS ₃	$2.73581 \cdot 10^5$	$2.73804 \cdot 10^5$
0.0234	0.55	0.15	366667	1.32408	$2.2746204 \cdot 10^{-5}$	CS ₄	$1.49867 \cdot 10^4$	$1.49874 \cdot 10^4$

Table 4: Main parameters for second frequency couple $10^{10}\text{Hz}/10^5\text{Hz}$ of tubulin.

RRM Frequency	Radio frequency range (Microwave) ν 10^{10} Hz (Pang)	Radio frequency range (Long waves) ν_0 10^5 Hz (Ichinose)	$m=\nu/\nu_0$	D (A°)	$\Delta E=mh\nu_0$ (eV)	Tier	$K_{T=298}$	$K_{T=314}$
0.0957	0.85	0.61	139344	2.14786	$3.5153224 \cdot 10^{-5}$	CS ₄	$6.09166 \cdot 10^4$	$6.09208 \cdot 10^4$
0.3320	3.85	2.12	181604	1.88143	$1.5922343 \cdot 10^{-4}$	CS ₄	$2.10690 \cdot 10^5$	$2.10756 \cdot 10^5$
0.4346	3.85	2.78	138489	2.15448	$1.5922343 \cdot 10^{-4}$	CS ₄	$2.76282 \cdot 10^5$	$2.76369 \cdot 10^5$
0.0234	0.25	0.15	166667	1.96393	$1.0339184 \cdot 10^{-5}$	CS ₄	$1.4994 \cdot 10^4$	$1.49943 \cdot 10^4$

unimolecular reaction rates for physiological temperatures of 298 K and 314 K. They vary greatly from 10^{-23} Hz to 10^6 Hz. For example, row 1 of Table 1 presents a CS₁-tier chemical reaction that is likely a tubulin polymerization [26,27]. In general, the calculated reaction rates can be divided into two ranges. Ultraslow reactions with reaction rates from 10^{-23} Hz to 10^{-14} Hz are apparently associated with cell division. Normal ones with reaction rates from 10^1 Hz to 10^6 Hz describe tubulin transformations. It is known that labile (that is, forming and then disintegrating) microtubules are found most often in

the cell cytoplasm [27]. This is the reason for the diversity of chemical reactions.

Telomerases and telomeres

These proteins protect the end of the chromosome from DNA damage or from fusion with neighboring chromosomes. Several groups of them were studied in [17] by means of the RRM model:

- (1) A first group consisted of five TERT telomerase proteins:



Q27ID4 – TERT_BOVIN, O14746 – TERT_HUMAN (1-230), O14746 – TERT_HUMAN (325-550), O70372 – TERT_MOUSE and Q673L6 – TERT_RAT.

- (2) A second one included six telomerase TERT mRNA coding sequences, Homo sapiens telomerase reverse transcriptase isoforms: JF896280.1 – Delta2, JF896283.1 – Delta2-8, JF896285.1 – Delta4-13, JF896281.1 – Delta3p-12, and JF896286.1 – INTR1.
- (3) A third one contained ten homo sapiens telomeric repeat region isolates: HQ167745.1 – AE, HQ167740.1 – DVW, HQ167744.1 – KA, HQ167746.1 – KM, HQ167741.1 – KP, HQ167742.1 – LH, HQ167748.1 – SA, HQ167747.1 – SE, HQ167743.1 – VDEC, and AF0207783.1 – chromosome 20.

The activation barrier characteristics are calculated as in the previous case. The results are presented in Tables 5–8. Row 11 of Table 5 fits the experimental data of [28]. Still, a thorough experimental data search remains to be done.

Ion channel proteins related to the pain transmission

Pain is a sensation associated with human suffering. Therefore, scientific research into its elimination is a priority.

In [18], the RRM model was used to study pain transmission, which is an electrical signal along the nerve (axon). This electrical signal is formed by complex activation (opening and closing) of specific pain-related ion channels and the redistribution of electrically charged ions at the nerve cell membrane. The activity of sodium and calcium ion channels is the most critical for pain transmission along nerves. The authors of [18] analyzed human, mouse, and rat ion channels

only, as they are mostly investigated and mostly related to human pain. The following protein sequences were used: twelve sodium ion channel proteins related to pain; three pain toxin proteins that influence opening and closing of sodium ion channels; fifteen mu-conotoxin proteins that also influence opening and closing of sodium ion channels; eight calcium ion channel proteins related to pain and eight omega-conotoxin proteins that influence opening and closing of calcium ion channels. Two characteristic RRM frequencies were identified: $fn1=0.1465$ for sodium ion channels and $fc2=0.1021$ for calcium ones. When different modalities of charge transfer through the protein backbone were introduced, the resonant frequencies for sodium and calcium ion channels were estimated to be in various frequency ranges, including THz, GHz, MHz, and kHz. Then it was concluded that different modalities of charge transfer can produce different resonant frequencies, which are not necessarily related to the protein's biological function, but could be related to ion channel resonances in general.

The activation barrier characteristics are shown in Tables 9–12. These are the number of quantum subsystems forming a barrier, dipole moments values, barrier activation energies, what tiers they belong to, and reaction rates at several temperatures. Row 1 of Table 9 fits the experimental data of [29]. More experimental confirmations are expected to be found.

Discussion

The above-mentioned modalities are quasi-particles, namely phonons, excitons, and solitons. Nevertheless, since 1989, the RRM model supposes all resonances are electromagnetic in nature. Since the activation process model

Table 5: Main parameters for frequency couple 10^{14} Hz/ 10^9 Hz of telomerases and telomers.

RRM Frequency	Optical range (IR) ν 10^{14} Hz (Cosic)	Radio frequency range (Microwave) ν_0 10^9 Hz (Yomosa)	$m=\nu/\nu_0$	D (A°)	$\Delta E=mh\nu_0$ (eV)	Tier	$K_{T=298}$	$K_{T=314}$
a TERT(5)								
0.2930	3.035	1.2335	246048	1.61637	1.2551719	CS ₀	$7.30245 \cdot 10^{-13}$	$8.8132 \cdot 10^{-19}$
0.4191	4.245	1.766	240374	1.63534	1.7555934	CS ₀	$3.59939 \cdot 10^{-21}$	$1.17256 \cdot 10^{-19}$
0.0161	$1.65 \cdot 10^{13}$	$6.75 \cdot 10^7$	244444	1.62166	$6.8238611 \cdot 10^{-2}$	CS ₂	$4.73419 \cdot 10^6$	$5.42065 \cdot 10^6$
0.2778	3.875	1.1655	332475	1.65697	1.6025734	CS ₀	$9.19683 \cdot 10^{-19}$	$2.21145 \cdot 10^{-17}$
0.2525	2.66	1.4885	178703	1.89664	$1.76256 \cdot 10^{-19}$	CS ₀	$3.69775 \cdot 10^{-10}$	$3.2806 \cdot 10^{-9}$
b TERT m RNA(6) conversion								
0.3730	8.86	1.571	563972	1.06763	3.6642066	CS ₀	$1.68564 \cdot 10^{-53}$	$2.4235 \cdot 10^{-50}$
0.4014	4.21	1.69	249112	1.6064	1.7411185	CS ₀	$6.05237 \cdot 10^{-21}$	$1.91583 \cdot 10^{-19}$
0.4902	5.08	2.064	246124	1.61612	2.1009221	CS ₀	$6.07737 \cdot 10^{-27}$	$3.92837 \cdot 10^{-25}$
cTELOMERE(10)		10^9 Hz						
0.1875	1.94	7.895	245725	1.61743	$8.0232063 \cdot 10^{-1}$	CS ₁	$2.13024 \cdot 10^{-5}$	$1.04674 \cdot 10^{-4}$
0.1904	1.97	8.015	245789	1.61722	$8.1472765 \cdot 10^{-1}$	CS ₁	$1.33399 \cdot 10^{-5}$	$6.71822 \cdot 10^{-5}$
0.1768	1.83	7.445	245803	1.61718	$7.5682823 \cdot 10^{-1}$	CS ₁	$1.18117 \cdot 10^{-4}$	$5.30298 \cdot 10^{-4}$
0.1846	1.91	8.075	236533	1.64856	$7.8991361 \cdot 10^{-1}$	CS ₁	$3.53223 \cdot 10^{-5}$	$1.69343 \cdot 10^{-4}$


Table 6: Main parameters for frequency couple $10^{13}\text{Hz}/10^8\text{Hz}$ of telomerases and telomers.

RRM Frequency	Optical range (IR) ν 10^{13} Hz (Yomosa)	Radio frequency range (Short waves) ν_0 10^8 Hz (Ichinose)	$m=\nu/\nu_0$	D (\AA°)	$\Delta E=mh\nu_0$ (eV)	Tier	K_{T-298}	K_{T-314}
a TERT(5)								
0.2930	4.65	1.31	354962	1.34574	$1.9230881 \cdot 10^{-1}$	CS ₁	$7.327 \cdot 10^4$	$1.07213 \cdot 10^5$
0.4191	6.55	1.88	353723	1.34809	$2.7502228 \cdot 10^{-1}$	CS ₁	$4.19715 \cdot 10^3$	$7.24367 \cdot 10^3$
0.0161	$2.0 \cdot 10^{12}$	$7 \cdot 10^6$	285714	1.49998	$8.2713468 \cdot 10^{-3}$	CS ₂	$5.07239 \cdot 10^6$	$5.15032 \cdot 10^6$
0.2778	4.45	1.24	358871	1.33839	$1.8403747 \cdot 10^{-1}$	CS ₁	$9.57112 \cdot 10^4$	$1.37898 \cdot 10^5$
0.2525	5.6	1.58	354430	1.34675	$2.3159771 \cdot 10^{-1}$	CS ₁	$1.91362 \cdot 10^4$	$3.02996 \cdot 10^4$
b TERT m RNA(6) conversion								
0.3730	5.9	1.67	353293	1.34891	$2.4400473 \cdot 10^{-1}$	CS ₁	$1.24763 \cdot 10^4$	$2.02460 \cdot 10^4$
0.4014	6.35	1.795	353760	1.34802	$2.6261526 \cdot 10^{-1}$	CS ₁	$6.49666 \cdot 10^3$	$1.09396 \cdot 10^4$
0.4902	7.75	2.195	353075	1.34933	$3.2051469 \cdot 10^{-1}$	CS ₁	$8.33412 \cdot 10^2$	$1.57423 \cdot 10^3$
c TELOMERE(10)								
0.1875	3.0	8.35	359281	1.33762	$1.240702 \cdot 10^{-1}$	CS ₁	$6.65885 \cdot 10^5$	$8.51763 \cdot 10^5$
0.1904	3.0	8.55	350877	1.35355	$1.240702 \cdot 10^{-1}$	CS ₁	$6.81835 \cdot 10^5$	$8.72164 \cdot 10^5$
0.1768	2.8	8.15	343558	1.36789	$1.1579886 \cdot 10^{-1}$	CS ₁	$8.96926 \cdot 10^5$	$1.12862 \cdot 10^6$
0.1846	2.9	7.85	369427	1.31913	$1.1993453 \cdot 10^{-1}$	CS ₁	$7.35403 \cdot 10^5$	$9.32998 \cdot 10^5$

Table 7: Main parameters for first frequency couple $10^{10}\text{Hz}/10^5\text{Hz}$ of telomerases and telomers.

RRM Frequency	Radio frequency range (Microwave) ν 10^{10} Hz (Davydov)	Radio frequency range (Longwaves) ν_0 10^5 Hz (Ichinose)	$m=\nu/\nu_0$	D (\AA°)	$\Delta E=mh\nu_0$ (eV)	Tier	K_{T-298}	K_{T-314}
a TERT(5)								
0.2930	6.6	1.93	341969	1.37106	$2.7295444 \cdot 10^{-4}$	CS ₃	$1.90959 \cdot 10^5$	$1.91063 \cdot 10^5$
0.4191	9.35	2.755	339383	1.37628	$3.8668546 \cdot 10^{-4}$	CS ₃	$2.71383 \cdot 10^5$	$2.71591 \cdot 10^5$
0.0161	$2.5 \cdot 10^9$	$1.1 \cdot 10^4$	227273	1.68181	$1.0339184 \cdot 10^{-5}$	CS ₄	$1.09956 \cdot 10^4$	$1.09958 \cdot 10^4$
0.2778	6.2	1.83	338798	1.37746	$2.5641175 \cdot 10^{-4}$	CS ₃	$1.81182 \cdot 10^5$	$1.81274 \cdot 10^5$
0.2525	7.5	2.225	337079	1.38097	$3.1017551 \cdot 10^{-4}$	CS ₃	$2.19829 \cdot 10^5$	$2.19964 \cdot 10^5$
b TERT m RNA(6) conversion								
0.3730	8.35	2.455	340122	1.37478	$3.4532873 \cdot 10^{-4}$	CS ₃	$2.42221 \cdot 10^5$	$2.42387 \cdot 10^5$
0.4014	9.0	2.64	340909	1.37319	$3.7221061 \cdot 10^{-4}$	CS ₃	$2.60201 \cdot 10^5$	$2.60393 \cdot 10^5$
0.4902	$1.1 \cdot 10^{11}$	3.225	341085	1.37284	$4.5492407 \cdot 10^{-4}$	CS ₃	$3.16837 \cdot 10^5$	$3.17123 \cdot 10^5$
c TELOMERE(10)								
0.1875	4.2	1.235	340081	1.37486	$1.7369828 \cdot 10^{-4}$	CS ₄	$1.22667 \cdot 10^5$	$1.22710 \cdot 10^5$
0.1904	4.25	1.255	338645	1.37777	$1.7576612 \cdot 10^{-4}$	CS ₄	$1.24644 \cdot 10^5$	$1.24687 \cdot 10^5$
0.1768	3.95	1.165	339056	1.37694	$1.633591 \cdot 10^{-4}$	CS ₄	$1.15761 \cdot 10^5$	$1.15799 \cdot 10^5$
0.1846	4.1	1.215	337449	1.38022	$1.6956261 \cdot 10^{-4}$	CS ₄	$1.20700 \cdot 10^5$	$1.20741 \cdot 10^5$

has no use for quasi-particles, it can be considered as evidence of this fruitful hypothesis.

The use of quasi-particles as energy carriers in proteins has a number of problems associated with energy conversion. Let us consider two of them. The first one is photon-phonon energy conversion. There is a list of rather specific conditions for this conversion to take place:

- (1) Their wave vectors must coincide.
- (2) Photon's polarization vector is not perpendicular to the phonon's vibration vector of the electrical dipole moment.
- (3) The energy conservation law is fulfilled.
- (4) Most importantly, this occurs below the Debye


Table 8: Main parameters for second frequency couple $10^{10}\text{Hz}/10^5\text{Hz}$ of telomerases and telomers.

RRM Frequency	Radio frequency range (Microwave) ν 10^{10} Hz (Pang)	Radio frequency range (Long waves) ν_0 10^5Hz (Ichinose)	$m=\nu/\nu_0$	D (A°)	$\Delta E=mh\nu_0$ (eV)	Tier	$K_{T=298}$	$K_{T=314}$
a TERT(5)								
0.2930	2.65	1.93	137306	2.16375	$1.0959535 \cdot 10^{-4}$	CS ₄	$1.92178 \cdot 10^5$	$1.92220 \cdot 10^5$
0.4191	3.75	2.735	137112	2.16528	$1.5508775 \cdot 10^{-4}$	CS ₄	$2.71853 \cdot 10^5$	$2.71937 \cdot 10^5$
0.0161	$1.5 \cdot 10^9$	$1.1 \cdot 10^4$	136364	2.17121	$6.2035101 \cdot 10^{-4}$	CS ₄	$1.09973 \cdot 10^4$	$1.09975 \cdot 10^4$
0.2778	3.45	1.83	188525	1.84657	$1.4268073 \cdot 10^{-4}$	CS ₄	$1.81986 \cdot 10^5$	$1.82038 \cdot 10^5$
0.2525	2.15	2.225	96629.2	2.57927	$8.8916978 \cdot 10^{-5}$	CS ₄	$2.21731 \cdot 10^5$	$2.21770 \cdot 10^5$
b TERT m RNA(6) conversion								
0.3730	3.35	2.455	136456	2.17047	$1.3854506 \cdot 10^{-4}$	CS ₄	$2.44179 \cdot 10^5$	$2.44246 \cdot 10^5$
0.4014	3.55	2.64	134470	2.18645	$1.4681641 \cdot 10^{-4}$	CS ₄	$2.62495 \cdot 10^5$	$2.62571 \cdot 10^5$
0.4902	4.35	3.225	134884	2.18309	$1.4268073 \cdot 10^{-4}$	CS ₄	$3.20249 \cdot 10^5$	$3.20363 \cdot 10^5$
c TELOMERE(10)								
0.1875	1.7	1.235	137652	2.16103	$7.0306447 \cdot 10^{-5}$	CS ₄	$1.23162 \cdot 10^5$	$1.23180 \cdot 10^5$
0.1904	1.7	1.255	135458	2.17845	$7.0306447 \cdot 10^{-5}$	CS ₄	$1.25157 \cdot 10^5$	$1.25174 \cdot 10^5$
0.1768	1.6	1.165	137339	2.16348	$6.6170774 \cdot 10^{-5}$	CS ₄	$1.16200 \cdot 10^5$	$1.16215 \cdot 10^5$
0.1846	1.65	1.215	135802	2.17569	$6.8238611 \cdot 10^{-5}$	CS ₄	$1.21178 \cdot 10^5$	$1.21194 \cdot 10^5$

Table 9: Main parameters for frequency couple $10^{14}\text{Hz}/10^8\text{Hz}$ of proteins related to the pain transmission.

RRM Frequency	Optical range (IR) ν 10^{14} Hz (Cosic)	Radio frequency range (Microwave) ν_0 10^8 Hz (Yomosa)	$m=\nu/\nu_0$	D (A°)	$\Delta E=mh\nu_0$ (eV)	Tier	$K_{T=298}$	$K_{T=314}$
Sodium 0.1465	1.515	6.165	245742	1.61738	$6.26554 \cdot 10^{-1}$	CS ₁	$1.56166 \cdot 10^{-2}$	$5.4141 \cdot 10^{-2}$
Calcium 0.1021	1.055	4.3	245349	1.61867	$4.36314 \cdot 10^{-1}$	CS ₁	17.9677	42.7063

Table 10: Main parameters for frequency couple $10^{13}\text{Hz}/10^7\text{Hz}$ of proteins related to the pain transmission.

RRM Frequency	Optical range (IR) ν 10^{13} Hz (Yomosa)	Radio frequency Range (Short waves) ν_0 10^7 Hz (Ichinose)	$m=\nu/\nu_0$	D (A°)	$\Delta E=mh\nu_0$ (eV)	Tier	$K_{T=298}$	$K_{T=314}$
Sodium 0.1465	2.3	6.55	351145	1.35303	$9.51205 \cdot 10^{-2}$	CS ₂	$1.6127 \cdot 10^6$	$1.94772 \cdot 10^6$
Calcium 0.1021	1.6	4.55	351618	1.35206	$6.61708 \cdot 10^{-2}$	CS ₂	$3.4588 \cdot 10^6$	$3.94411 \cdot 10^6$

Table 11: Main parameters for first frequency couple $10^{10}\text{Hz}/10^4\text{Hz}$ related to the pain transmission of proteins.

RRM Frequency	Radio frequency range (Microwave) ν 10^{10} Hz (Davydov)	Radio frequency range (Long waves) ν_0 10^4 Hz (Ichinose)	$m=\nu/\nu_0$	D (A°)	$\Delta E=mh\nu_0$ (eV)	Tier	$K_{T=298}$	$K_{T=314}$
Sodium 0.1465	3.3	9.65	341969	1.37106	$1.36477 \cdot 10^{-4}$	CS ₄	9.5988510^4	$9.60145 \cdot 10^4$
Calcium 0.1021	2.3	6.7	343284	1.36844	$9.51205 \cdot 10^{-5}$	CS ₄	$6.67523 \cdot 10^4$	$6.67649 \cdot 10^4$



Table 12: Main parameters for second frequency couple 10^{10} Hz/ 10^4 Hz related to the pain transmission of proteins.

RRM Frequency	Radio frequency range (Microwave) ν 10^{10} Hz (Pang)	Radio frequency range (Long waves) ν_0 10^4 Hz (Ichinose)	$m=\nu/\nu_0$	D (\AA)	$\Delta E=mh\nu_0$ (eV)	Tier	$K_{T=298}$	$K_{T=314}$
Sodium 0.1465	1.3	9.65	134715	2.18445	$5.37638 \cdot 10^{-5}$	CS ₄	$9.62982 \cdot 10^4$	$9.63084 \cdot 10^4$
Calcium 0.1021	0.9	6.7	134328	2.1876	$3.72211 \cdot 10^{-5}$	CS ₄	$6.6903 \cdot 10^4$	$6.6979 \cdot 10^4$

temperature [23]. However, this temperature is lower than the physiological temperature of a mammalian cell.

According to Davydov, an exciton is a part of a soliton [30,31], so there is no need to consider it separately. The second problem is the thermal stability of solitons. It was first studied by Enrico Fermi, John Pasta, Stanislaw Ulam, and Mary Tsingou [32], and by Norman Julius Zabusky and Martin David Kruskal [33] later. However, considerable doubt arose concerning whether the Davydov soliton is sufficiently stable in the region of biological temperature to provide a viable explanation for bio-energy transport in protein alpha-helices [34,35]. Several solutions to this problem were proposed.

It was shown that Davydov solitons are able to quantum tunnel through massive barriers or to quantum interfere at collision sites by consuming up to four amide I energy quanta [36]. As this took place, both solitons' thermal stability and lifetimes increased. Another computational simulation demonstrated that the cooperative action of three amide I exciton quanta in the full protein alpha-helix ensured a soliton lifetime of over 30 ps, during which the amide I energy could be transported along the entire extent of an 18-nm-long alpha-helix at $T=310$ K [13]. Since the hydrolysis of a single adenosine triphosphate molecule can initiate three amide I exciton quanta, it was concluded that proteins could harness soliton-assisted energy transport at physiological temperature.

On the other hand, Pang Xiao-Heng improved and developed the Davydov model drastically [35]. Davydov's wave function was replaced with a quasi-coherent two-quanta state to exhibit the coherent behaviors of collective excitations, which are a feature of the energy released in ATP hydrolysis in the systems. The new interaction term was added to Davydov's Hamiltonian to represent the correlations of the collective excitations and collective motions in protein molecules. As a result, the binding energy of the new soliton was 23 times larger than that of the Davydov soliton, and it could travel at supersonic speed. Thus, the new soliton had a large lifetime and good thermal stability in the region of biological temperature.

With these investigations, it is possible to say that solitons provide energy transport in protein alpha-helices. However, the mechanism for this process in protein beta-sheets and beta-turns is unknown. So, the theory of energy transfer in proteins is still far from accurate.

Conclusions

The results of this report can be summarized as follows:

- (1) The resonant recognition model frequencies for tubulins, several telomerases, and telomeres, and ion channel proteins related to the pain transmission are explained by means of the activation process model.
- (2) The resonant electromagnetic frequencies are estimated to be in various frequency ranges, including THz, GHz, MHz, and kHz. They are associated with activation processes for various CS tiers of protein energy landscapes.
- (3) Several activation processes have experimental confirmation.
- (4) Protein primary, secondary, and tertiary structural changes can be better understood using the activation process model, since it has no use for quasi-particles.
- (5) The proposed model may become the basis for a protein folding explanation.

References

1. Geesink HJH, Meijer DKF. Quantum wave information of life revealed: an algorithm for electromagnetic frequencies that create stability of biological order, with implications for brain function and consciousness. *NeuroQuantology*. 2016;14(1):106–125. Available from: <https://doi.org/10.14704/nq.2016.14.1.911>
2. Geesink HJH, Meijer DKF. Bio-soliton model that predicts distinct non-thermal electromagnetic radiation frequency bands that either stabilize or destabilize life conditions. *Electromagn Biol Med*. 2016. Available from: <https://doi.org/10.1080/15368378>
3. Cosic I, Vojisavljevic V, Pavlovic M. The relationship of the resonant recognition model to the effects of low-intensity light on cell growth. *Int J Radiat Biol*. 1989;56(2):179–191. Available from: <https://doi.org/10.1080/09553008914551131>
4. Cosic I, Fang A. Prediction of protein active site using signal processing methods. In: 2nd International Conference on Bioelectromagnetism; 1998 Feb; Melbourne, Australia. p. 69–70. Available from: <https://doi.org/10.1109/ICBEM.1998.666399>
5. Bandyopadhyay A, Ray K. Rhythmic oscillation in proteins to human cognition. *Cham: Springer*; 2021. doi:10.1007/978-981-15-7253-1. Available from: <https://doi.org/10.1007/978-981-15-7253-1>
6. Meijer DKF, Geesink HJH. Phonon guided biology: architecture of life and conscious perception are mediated by toroidal coupling of phonon, photon and electron information fluxes at discrete eigenfrequencies. *NeuroQuantology*. 2016;14(4):718–755. Available from: https://www.researchgate.net/publication/311869830_Phonon_Guided_Biology_Architecture_of_Life_and_Conscious_Perception_Are_Mediated_by_Toroidal_Coupling_of_Phonon_Photon_and_Electron_Information_Fluxes_at_Discrete_Eigenfrequencies



7. Ciblis P, Cosić I. The possibility of soliton/exciton transfer in proteins. *J Theor Biol.* 1997;184:331–338. Available from: <https://doi.org/10.1006/jtbi.1996.0285>
8. Cosić I. Macromolecular bioactivity: is it resonant interaction between macromolecules? *IEEE Trans Biomed Eng.* 1994;41(12):1101–1114. Available from: <https://doi.org/10.1109/10.335860>
9. Cosić I. The resonant recognition model of biomolecular interactions: possibility of electromagnetic resonance. *Pol J Med Phys Eng.* 2001;7(1):73–87.
10. Nienhaus GU, Müller JD, McMahon BH, Frauenfelder H. Exploring the conformational energy landscape of proteins. *Physica D.* 1997;107:297–311. Available from: [https://doi.org/10.1016/S0167-2789\(97\)00089-3](https://doi.org/10.1016/S0167-2789(97)00089-3)
11. Leeson DT. Exploring protein energy landscapes [dissertation]. University of Groningen; 1997. Available from: https://pure.rug.nl/ws/portalfiles/portal/13935578/0_full.pdf
12. Stepanov AV. Interaction model of thermal radiation with molecule at low temperatures: molecular tunnelling. *J Mol Struct Theochem.* 2002;578:47–61. Available from: [https://doi.org/10.1016/S0166-1280\(01\)00539-3](https://doi.org/10.1016/S0166-1280(01)00539-3)
13. Georgiev DD, Glazebrook JF. Thermal stability of solutions in protein α -helices. *arXiv:2202.00525.* 2022. Available from: <https://arxiv.org/abs/2202.00525>
14. Krupyanskiy YF, Gol'danskii VI. Dynamical properties and energy landscape of simple globular proteins. *Usp Fiz Nauk.* 2002;172(11):1247–1269.
15. Sahu S, Ghosh S, Ghosh B, Aswani K, Hirata K, Fujita D, Bandyopadhyay A. Atomic water channel controlling remarkable properties of a single brain microtubule. *Biosens Bioelectron.* 2013;47:141–148. Available from: <https://doi.org/10.1016/j.bios.2013.02.032>
16. Cosić I, Lazar K, Cosić D. Prediction of tubulin resonant frequencies using the resonant recognition model. *IEEE Trans Nanobioscience.* 2015;14:1–7. Available from: <https://doi.org/10.1109/TNB.2014.2365851>
17. Cosić I, Cosić D, Lazar K. Is it possible to predict electromagnetic resonances in proteins, DNA, and RNA? *EPJ Nonlinear Biomed Phys.* 2015;3:5. Available from: <https://doi.org/10.1140/s40366-015-0020-6>
18. Cosić I, Cosić D. Influence of tuning element relief patches on pain as analyzed by the resonant recognition model. *IEEE Trans Nanobioscience.* 2017;16(8):822–827. Available from: <https://doi.org/10.1109/TNB.2017.2696938>
19. Tavgin VL, Stepanov AV. Activation process model. *Phys Status Solidi B.* 1990;161:123–130. Available from: <https://doi.org/10.1002/pssb.2221610114>
20. Tavgin VL, Stepanov AV. Activation process model: application for diffusivity in covalent crystals. *J Mol Struct Theochem.* 1992;257:1–24. Available from: https://scholar.google.com/citations?view_op=view_citation&hl=ru&user=Zqk_iFoAAAAJ&citation_for_view=Zqk_iFoAAAAJ:u-x6o8ySG0sC
21. Stepanov AV, Tavgin VL. Development of the activation process model: compensation effect. *Int J Quantum Chem.* 1996;59:7–14. Available from: [https://doi.org/10.1002/\(SICI\)1097-461X\(1996\)59:1](https://doi.org/10.1002/(SICI)1097-461X(1996)59:1)
22. Stepanov AV. Activation process model: Einstein coefficients for activation barrier. *J Mol Struct Theochem.* 2007;805:87–92. Available from: https://scholar.google.com/citations?view_op=view_citation&hl=ru&user=Zqk_iFoAAAAJ&citation_for_view=Zqk_iFoAAAAJ:u5HHmVD_u08C
23. Stepanov AV. Modeling of metamaterials: a globular protein as a metamaterial prototype for electromagnetic–acoustic conversion at low temperatures. *Proc SPIE.* 2011;8070:807013. Available from: <https://doi.org/10.1117/12.886592>
24. Stepanov AV. Information entropy of activation process: application for low-temperature fluctuations of a myoglobin molecule. *Int J Mod Phys B.* 2015;29:1550016. <https://doi.org/10.1142/S0217979215500162>
25. Stepanov AV, Stepanov MA. Negative entropy production in L-lactate dehydrogenase kinetics. *Arch Biochem.* 2023;6(1):1–9. Available from:
26. Li G, Moore JK. Microtubule dynamics at low temperature: evidence that tubulin recycling limits assembly. *Mol Biol Cell.* 2020;31:1154–1166. Available from: <https://doi.org/10.1091/mbc.E19-10-0573>
27. Metzler DE. *Biochemistry: the chemical reactions of living cells.* Vol 1. Moscow: Mir; 1980.
28. Sayed ME, Cheng A, Yadav GP, Ludlow AT, Shay JW, Wright WE, Jiang QX. Catalysis-dependent inactivation of human telomerase and its reactivation by intracellular telomerase-activating factors. *J Biol Chem.* 2019;294(30):11579–11596. Available from: <https://doi.org/10.1074/jbc.RA119.008479>
29. Kriegeskorte S, Bott R, Hampl M, Korngreen A, Hausmann R, Lampert A. Cold and warmth intensify pain-linked sodium channel gating effects and persistent currents. *J Gen Physiol.* 2023;155(9):1–21. Available from: <https://doi.org/10.1085/jgp.202313207>
30. Davydov AS. *Solid state physics.* Moscow: Nauka; 1976.
31. Davydov AS. Solitons in quasi-one-dimensional molecular chains. *Usp Fiz Nauk.* 1982;138(4):603–643.
32. Fermi E, Pasta J, Ulam S. Studies of nonlinear problems. *Los Alamos Rep.* 1955;266:490–501. <https://doi.org/10.2172/4376203>
33. Zabusky NJ, Kruskal MD. Interaction of solitons in a collisionless plasma. *Phys Rev Lett.* 1965;15(6):240–243. Available from: <https://doi.org/10.1103/PhysRevLett.15.240>
34. Austin RH, Xie A, Fu D, Warren WW, Redlich B, van der Meer L. Tilting after Dutch windmills: probably no long-lived Davydov solitons in proteins. *J Biol Phys.* 2009;35:91–101. Available from: <https://doi.org/10.1007/s10867-008-9108-2>
35. Pang XF. The bio-energy transport in protein molecules and experimental validations. *Ann Proteomics Bioinformatics.* 2018;2:1–48. Available from: <https://doi.org/10.15761/APB.1000102>
36. Georgiev DD, Glazebrook JF. Quantum transport and utilization of free energy in protein α -helices. *arXiv:2003.13814.* 2020. Available from: <https://arxiv.org/abs/2003.13814>

Discover a bigger Impact and Visibility of your article publication with Peertechz Publications

Highlights

- ❖ Signatory publisher of ORCID
- ❖ Signatory Publisher of DORA (San Francisco Declaration on Research Assessment)
- ❖ Articles archived in worlds' renowned service providers such as Portico, CNKI, AGRIS, TDNet, Base (Bielefeld University Library), CrossRef, Scilit, J-Gate etc.
- ❖ Journals indexed in ICMJE, SHERPA/ROME0, Google Scholar etc.
- ❖ OAI-PMH (Open Archives Initiative Protocol for Metadata Harvesting)
- ❖ Dedicated Editorial Board for every journal
- ❖ Accurate and rapid peer-review process
- ❖ Increased citations of published articles through promotions
- ❖ Reduced timeline for article publication

Submit your articles and experience a new surge in publication services <https://www.peertechzpublications.org/submit>

Peertechz journals wishes everlasting success in your every endeavours.